



# Targeting of sialoadhesin-expressing macrophages through antibody-conjugated (polyethylene glycol) poly(lactic-co-glycolic acid) nanoparticles

Sofie Van Hees · Kimberley Elbrink · Marjorie De Schryver · Peter Delputte · Filip Kiekens

Received: 16 October 2021 / Accepted: 28 February 2022 / Published online: 14 March 2022  
© The Author(s), under exclusive licence to Springer Nature B.V. 2022

**Abstract** This research aims to evaluate different-sized nanoparticles consisting of (polyethylene glycol) (PEG) poly(lactic-co-glycolic acid) (PLGA), loaded with fluorescein isothiocyanate for nanoparticle uptake and intracellular fate in sialoadhesin-expressing macrophages, while being functionalized with anti-sialoadhesin antibody. Sialoadhesin is a macrophage-restricted receptor, expressed on certain populations of resident tissue macrophages, yet is also upregulated in some inflammatory conditions. The nanocarriers were characterized for nanoparticle size (84–319 nm), zeta potential, encapsulation efficiency, and in vitro dye release. Small (86 nm) antibody-functionalized PEG PLGA nanoparticles

showed persisting benefit from sialoadhesin-targeting after 24 h compared to the control groups. For small (105 nm) PLGA nanoparticles, uptake rate was higher for antibody-conjugated nanoparticles, though the total amount of uptake was not enhanced after 24 h. For both plain and functionalized small-sized (PEG) PLGA nanoparticles, no co-localization between nanoparticles and (early/late) endosomes nor lysosomes could be observed after 1-, 4-, or 24-h incubation time. In conclusion, decorating (PEG) PLGA nanocarriers with anti-sialoadhesin antibodies positively impacts macrophage targeting, though it was found to be formulation-specific.

**Keywords** PEG PLGA · PLGA · Nanoparticle · Targeting · Sialoadhesin · Macrophage · Drug delivery

## Introduction

Recently, the targeting of different cell types or tissues has been a broadly applied technique in nanomedicine to ensure safe and adequate administration of desired compounds (Patra et al. 2018). Amongst those targets, macrophages appear to be ideal candidates for particle-based drug delivery systems due to their phagocytic properties (Pei and Yeo 2016). Nanoparticles (NPs) are easily transformable by ligand conjugation to their outer surface and are widely exploited in macrophage-related diseases (Gaspar

---

S. Van Hees · K. Elbrink · F. Kiekens (✉)  
Department of Pharmaceutical Sciences, Laboratory for Pharmaceutical Technology and Biopharmacy, University of Antwerp, Universiteitsplein 1, 2610 Wilrijk, Belgium  
e-mail: Filip.Kiekens@uantwerpen.be

S. Van Hees  
e-mail: Sofie.VanHees@uantwerpen.be

K. Elbrink  
e-mail: Kimberley.Elbrink@uantwerpen.be

M. De Schryver · P. Delputte  
Department of Biomedical Sciences, Laboratory for Microbiology, Parasitology and Hygiene, University of Antwerp, Universiteitsplein 1, 2610 Wilrijk, Belgium  
e-mail: marjoriesdeschryver@hotmail.com

P. Delputte  
e-mail: Peter.Delputte@uantwerpen.be

et al. 2019). Frequently targeted receptors for macrophages are, for example, the mannose receptor and Fc receptor by binding respectively carbohydrates or antibodies to the NP surfaces (Kelly et al. 2011). Nanoparticle (NP) uptake was proven to be enhanced with the addition of targeting ligands compared to undecorated particles. However, several receptors (such as the mannose receptor) may also be found on other cell types such as endothelial cells, fibroblasts, and other immune cells (Hu et al. 2018). Moreover, macrophages are a very diverse group of cells where polarization through macrophage activation can result in particular phenotypes, which are able to perform various functions throughout the body. Therefore, a more specific targeting system might be in place (Jain et al. 2013). This research focused on sialoadhesin (Sn)-expressing macrophages, as this specific subpopulation has been demonstrated to be involved in inflammatory diseases, such as rheumatoid arthritis, associated with cancer and has shown potential for vaccine development strategies (O'Neill et al. 2013). Therefore, targeting Sn-expressing macrophages with anti-inflammatory-loaded or toxic carriers could be an attractive strategy in controlling these conditions, while avoiding possible toxic side effects of the drug by potentially lowering the dose.

Sn, also known as Siglec-1 or CD169, is considered to be a macrophage-restricted receptor and is found principally in inflammatory and some resident macrophages, for instance, in secondary lymphoid organs spleen and lymph nodes, bone marrow, liver, lungs, and gut (colon) (O'Neill et al. 2013; Asano et al. 2018; Ohnishi et al. 2013; Klaas and Crocker 2012). As a member of the sialic acid-binding Ig-like lectins (Siglecs), this receptor recognizes sialylated ligands expressed on, for example, activated lymphocytes, erythrocytes, apoptotic cells, and pathogens (Hartnell et al. 2001). The main function of Sn is not fully established, but is associated with regulation of the immune system and in addition the establishment of cell–cell interactions as well as cell–matrix interactions (Klaas and Crocker 2012).

Sn was previously identified as an endocytic receptor that already has been used for immunotargeting (Ooms et al. 2013a, b; Delputte et al. 2011; De Schryver et al. 2016). Yet, initially, it was not considered to be an endo- or phagocytic receptor, as red blood cells that bound to the receptor via sialic acids were not phagocytized (O'Neill et al. 2013).

However, Sn-dependent uptake of *Neisseria meningitidis* (Jones et al. 2003) and endocytosis of sialylated enveloped viruses (Klaas and Crocker 2012; Ooms et al. 2013b) were shown later on, as well as uptake of high-affinity glycan ligand-functionalized and GM3-targeted liposomes (Chen et al. 2012; Nijen Twilhaar et al. 2020). Therefore, Sn could indeed be involved in endo- and phagocytic uptake, under specific circumstances (Klaas and Crocker 2012).

To study the targeting of Sn-expressing macrophages, fluorescein isothiocyanate (FITC) was incorporated into (PEG) PLGA NPs to determine the difference in the amount of uptake of equivalent masses of functionalized and control NPs by means of flow cytometry. The intracellular fate of the best formulation was assessed through confocal fluorescence microscopy. (PEG) PLGA was chosen because of its biocompatible and biodegradable properties (Elmowafy et al. 2019). Moreover, ligand binding is quite straightforward due to the carboxylic end groups of the polymers using carbodiimide chemistry (Wagh and Law 2013). At last, polymeric NP size is readily adaptable by varying different process parameters such as the concentration of stabilizer (Vandervoort and Ludwig 2002).

## Materials and methods

### Materials

PLGA: Resomer® RG 503 H [lactide:glycolide 50:50, carboxyl-terminated, MW 24,000–38,000] was produced by Boehringer Ingelheim (Ingelheim am Rhein, Germany). PEG PLGA: A1171 [lactide:glycolide 50:50, carboxyl-terminated, MW 30,000, 5000 Da] was purchased from PolySciTech (Akina Inc., West Lafayette, IN, USA). Fluorescein isothiocyanate (FITC), dichloromethane (DCM), cell reagents (RPMI/IMDM cell medium, Accumax® etc.), fixative-free lysing solution, tetramethyl rhodamine isothiocyanate (TRITC)-donkey anti-rat secondary antibody, and Texas Red-X® phalloidin were acquired from Thermo Fisher Scientific (Merelbeke, Belgium). Dimethyl sulfoxide (DMSO), ethyl acetate (EA), polyvinyl alcohol (PVA) [MW 31,000–50,000, 87–89% hydrolyzed], N-(3-dimethylaminopropyl)-N'-ethyl carbodiimide hydrochloride (EDC), N-hydroxysuccinimide (NHS), Triton X-100,

4',6-diamidino-2-phenylindole (DAPI), and 1,4-diazabicyclo[2.2.2]octane (DABCO) were provided by Sigma-Aldrich (Overijse, Belgium). Disodium hydrogen phosphate dihydrate, sodium dihydrogen phosphate dihydrate, and paraformaldehyde were bought from Merck GmbH (Overijse, Belgium). Polyclonal antibodies conjugated to 555 Alexa Fluor against Early Endosome Antigen 1 (EEA1), cation-independent mannose-6-phosphate (CI M6P), and cathepsin B were acquired from Bio-connect (Huissen, The Netherlands). Mannitol was obtained from Duchefa Farma (Haarlem, The Netherlands), sodium chloride from Carl Roth GmbH (Karlsruhe, Germany), normal rat IgG control and mouse IFN-alpha from Bio-Techne Ltd (R&D Systems/Tocris) (Oxfordshire, UK), and Bio-Rad Protein Assay Kit from Bio-Rad Laboratories (Temse, Belgium). L929 murine fibroblast cell line was kindly provided by Dr. C. Uyttenhove (Ludwig Institute for Cancer Research, Brussels, Belgium), and CHO-K1 cells by Dr. J. D. Esko (University of California, San Diego, CA, USA).

## Methods

### *Preparation of nanoparticles*

(PEG) PLGA NPs (polymers AII71 or Resomer® RG 503 H) were prepared by means of the oil-in-water (O/W) emulsion solvent evaporation method, followed by freeze-drying for long-term storage. FITC was encapsulated as a fluorescent marker.

Initially, 100 mg of (PEG) PLGA was dissolved in 4 mL of EA. FITC was dissolved in DMSO at a concentration of 1 mg/mL and 1 mL of FITC solution was added to the organic phase. Thereupon, 10 mL of an external water phase, containing either 0.2%, 2%, or 4% (w/w) PVA in ultrapure water (Direct pure adept, Reophile Bioscience Ltd., (Belgium)) was added and the mixture was emulsified by ultrasonication (1 min, amplitude 20%) (VIBRA CELL VCX-750, 6-mm probe, Sonics, USA). The resulting O/W emulsions were magnetically stirred (700 rpm) at room temperature for 24 h to allow the evaporation of the solvent (EA). The produced NPs were washed three times at  $20,000\times g$  by means of centrifugation until supernatant was clear (Sigma 4–16 KS, Sigma Laborzentrifugen GmbH, Germany). Finally, the NPs were added to 0.2 g mannitol as a cryoprotectant,

lyophilized at standard conditions for at least 72 h (FreeZone® 1 L benchtop freeze dry system, Labconco, USA) and stored at 2–8 °C in a plastic container protected from light until further use. Blank NPs were prepared accordingly without addition of FITC.

### *Characterization of nanoparticles*

The yield (particle concentration, expressed as mass PLGA NPs per mass freeze-dried powder in percentage) of each sample was determined by weighing samples after freeze-drying, taking the amount of mannitol weighed prior to freeze-drying into account.

NP size distributions of freeze-dried samples were measured in ultrapure water through dynamic light scattering (DLS) (Zetasizer Nano-ZS, Malvern Instruments, UK) and laser diffraction (LD) (Mastersizer 3000, Malvern Instruments, UK). DLS results were expressed as the mean NP hydrodynamic diameter (Z-Ave (nm)) and size distributions were characterized by the polydispersity index (PdI) as a measure for the width of the distribution. The median NP size (dx(50)) calculated by number density (%) was measured through LD.

Zeta potential was determined through electrophoretic light scattering (ELS) (Zetasizer Nano-ZS). NPs were redispersed in ultrapure water and results were calculated as the average of three measurements for each sample.

The encapsulation efficiency (EE) of FITC was analyzed by means of a spectrophotometric assay (Specord 200 plus, Analytik Jena AG, Germany).

The FITC standard curve in phosphate-buffered saline (PBS) (pH 7.4) showed good linearity ( $R^2 > 0.999$ ); linear range was 1 to 8  $\mu\text{g/mL}$  measured at 495-nm wavelength. Equivalent amounts of freeze-dried powder containing 2 mg of PLGA NPs were accurately weighed in triplicate, reconstituted in 1 mL PBS (pH 7.4) and 1 mL DCM, and vortexed regularly. FITC containing aqueous solution was collected after standing overnight and centrifuged ( $20,000\times g$  for 10 min). Considering the color, FITC concentrations in the DCM fraction were negligible. Each sample was measured three times at 495 nm.

The EE in the NP formulations was calculated employing the following equation:

$$EE (\%) = \frac{\text{Measured amount of compound}}{\text{Theoretical amount of compound}} * 100\%$$

The drug/dye loading (DL) is defined as

$$DL (\%) = \frac{\text{Measured amount of compound}}{\text{Weighted amount of PLGA NPs}} * 100\%$$

In vitro dye release studies were performed as well. In order to quantify the amount of FITC released from PLGA NPs, an equivalent of freeze-dried sample containing 6 mg of PLGA NPs was accurately weighed in triplo for each time point, transferred to a microtube, and dispersed into 1 mL PBS (pH 7.4). The microtubes were moved in a water bath at  $37 \pm 1$  °C and at specified time intervals (0 min, 5 min, 15 min, 30 min, 60 min, 120 min, 180 min, 300 min, 420 min, 1440 min); the samples were centrifuged at  $20,000 \times g$  for 10 min, after which the FITC concentration in the supernatant was determined using the same spectrophotometric method as described for the EE above.

#### *Antibody production and conjugation*

SySy94 hybridoma cells (De Schryver et al. 2016) were cultivated in IMDM cell medium with 20% iFCS. Cells were brought in a T150 culture flask with IMDM cell medium without iFCS containing 1% ITSX and 1% sodium pyruvate for antibody production. After a week, cell medium containing secreted SySy94 antibodies (targeting murine Sn) was purified using chromatography (AktaPrime plus, GE Healthcare) over a HiTrap Protein G HP column (GE Healthcare, USA) and concentrated on an Amicon® spin column 100 kDa cutoff (Fisher Scientific, Belgium). Diluted mAb solutions (1.5 mg/mL) were frozen at  $-80$  °C until further use.

To validate the specificity of the produced antibodies, a recombinant sialoadhesin-expressing CHO cell line (CHO-mSn) and wildtype CHO cell line (CHO-K1) were cultivated (De Schryver et al. 2016). Cells were seeded in a 24-well plate at a concentration of  $2 \times 10^5$  cells/well and incubated for 24 h at 37 °C to allow adherence on a glass coverslip. Cells were fixed with 4% (w/v) paraformaldehyde, the primary antibody SySy94 was incubated with the fixed cells for 1 h at 37 °C, the cells were washed, and the secondary TRITC donkey anti-rat antibody was added to the cells and incubated for

1 h at 37 °C. After washing and nucleus staining with DAPI, the coverslips were placed on a droplet of DABCO on a microscopic slide and stored at 4 °C. The analysis of the microscopic slides was performed with an Axio Observer inverted fluorescence microscope connected to a Compact Light Source HXP 120C with filter sets 49, 20, and 10 for blue, red, and green fluorophores respectively (Carl Zeiss Microscopy, Germany).

NPs were conjugated to either SySy94 antibodies or rat IgG isotype control antibodies through carbodiimide chemistry, following the protocol of Wagh and Law (Wagh and Law 2013). In brief, 10 mg of NPs was weighed and dispersed in 5 mL of PBS (pH 7.4). 250 µL of EDC solution (5.2 µmol) and NHS solution (8.7 µmol) in PBS (pH 7.4) was added and the mixture was agitated for 4 h at room temperature. NPs were washed three times with PBS (pH 7.4) by means of centrifugation ( $20,000 \times g$ , 30 min, 4 °C). Then, NPs were dispersed in 2 mL PBS (pH 7.4) and 500 µL of a 100 µg/mL SySy94 solution was added, agitated for 2 h at room temperature, and kept overnight at 4 °C. Antibody-conjugated NPs were repeatedly washed by centrifugation, and supernatant was kept for the determination of the conjugation efficiency. Control NPs were subjected to the same protocol, without the addition of antibodies. Quantification of mAb amounts on the NP surface was evaluated indirectly by determining the remaining mAb concentration using the Bio-Rad protein assay kit according to the manufacturer's instructions. Briefly, the conjugation efficiency (CE) of mAb to the NPs was analyzed by means of a spectrophotometric assay based on the binding of the Coomassie® Brilliant Blue G-250 dye and the amino residues of certain amino acids, causing a shift in the absorbance maximum. The IgG standard curve in phosphate-buffered saline (PBS) (pH 7.4) showed good linearity ( $R^2 > 0.997$ ), and the linear range was 2.5 to 25 µg/mL measured at 595-nm wavelength. Supernatant, consisting of unbound antibody and PBS (pH 7.4), was diluted 10 times. 800 µL of the standard solutions or the diluted supernatant was added to 200 µL of the dye concentrate, vortexed, and incubated for 10 min at room temperature. Each sample was prepared in duplo and each duplicate was measured three times.

The CE of the NP formulations was calculated employing the following equation:

$$CE (\%) = \frac{\text{Measured amount of IgG in supernatant}}{\text{Theoretical amount of IgG in supernatant}} * 100\%$$

### *In vitro cell experiments*

Sacrificed control female Swiss mice from experiments that were authorized by the Ethical Committee for Animals of the University of Antwerp, permit number 2019–10, were used to collect primary cells.

Primary bone marrow-derived macrophages from euthanized control female Swiss mice were collected by flushing the femur and tibia with RPMI medium. After removing red blood cells with a fixative-free lysis buffer, macrophages were counted and seeded in a 24-well plate at a concentration of  $2 \times 10^5$  cells/well or a 96-well plate at a concentration of  $5 \times 10^4$  cells/well. RPMI cell medium enriched with 10% (v/v) iFBS, 1% (v/v) non-essential amino acids, 1% (v/v) sodium pyruvate, 1% (v/v) glutamine, and 10% (v/v) L929 supernatant was added after 1 to 6 h and refreshed after another 24 h of incubation time. On day 6, macrophages were stimulated with mouse IFN- $\alpha$  (100 IU/mL) to induce Sn expression (De Schryver et al. 2017a, b). Macrophages were cultured for 7 days in total before endocytosis experiments were performed.

For flow cytometry experiments, conjugated and control NPs were dispersed in cooled enriched RPMI cell medium and sonicated for 15 min to enhance reconstitution in cell medium. 300  $\mu$ L of NP dispersion with (a) concentration(s) of 0.5 mg/mL (and 1 mg/mL and 1.5 mg/mL for 24 h) was added to the cells in the 24-well plate. After 1, 4, or 24 h, cells were washed three times with PBS, partially dissociated with Accumax® for 30 min, fixed with 4% (w/v) paraformaldehyde, and detached from the plate with a cell scraper for flow cytometry analysis. The experiment was performed in triplicate. The average fluorescence of 5000 cells was measured using an Attune NxT Flow Cytometer (Thermo Fisher Scientific, Singapore), with excitation from a blue laser (488 nm) and detection through FSC, SSC, and the first fluorescent channel (BL1). Outcomes were mean fluorescence intensity (MFI) as a measure for cellular NP uptake and the number of fluorescent cells (%) (cutoff value of a “fluorescent cell”:  $MFI > 2 \times 10^3$ ).

For fluorescence microscopy experiments, cells were seeded in a 96-well plate suited for imaging in a

concentration of  $5 \times 10^4$  cells/well. 65  $\mu$ L of a 0.8 mg/mL NP suspension was added to the cells and incubated at 37 °C for 1, 4, or 24 h. Macrophages were then washed three times with PBS (pH 7.4), fixed with 4% (w/v) paraformaldehyde, permeabilized with Triton X-100, and colored with polyclonal antibodies conjugated to Alexa Fluor 555 against EEA1, CI M6P, and cathepsin B to visualize endosomes, late endosomes, and lysosomes respectively and DAPI to stain cell nuclei. DABCO solution was added as mounting medium to preserve fluorescent properties. Fluorescent images were obtained with a Leica SP8 laser confocal scanning microscope equipped with a Leica HyD detector (Leica microsystems, Germany).

### *Statistical analysis*

The results of the endocytosis experiments were calculated as the mean and standard deviation of three measurements. For 1-h and 4-h assays, one-way ANOVA (SPSS) with Tukey HSD post hoc testing was used to identify significant differences ( $p$ -value  $< 0.05$ ) between groups. For the 24-h assay, a general linear regression model based on the analysis of variances with Tukey HSD post hoc testing, including the independent variables “functionalization” and “concentration,” was performed to determine significant effects ( $p$ -value  $< 0.05$ ). The level of significance is represented in the figures with asterisks whereby 1 asterisk stands for a  $p$ -value  $\leq 0.05$ , 2 for  $p \leq 0.01$ , 3 for  $p \leq 0.001$ , and 4 for  $p \leq 0.0001$ .

## **Results**

### *Nanoparticle characteristics*

An overview of NP characteristics of all formulations is presented in Table 1. As expected, NP size decreased with increasing concentration of the PVA stabilizer in the outer water phase during production of the NPs. All formulations showed size distributions in the nanometer range. It should be noted that initial PdI was small; however, after washing and freeze-drying of the NPs, both Z-Ave and PdI were elevated (especially for 4% PEG PLGA NPs, e.g., 142 nm PdI 0.168 before vs. 368 nm PdI 0.410 after). NP formulations showed negative zeta potential values when measured in ultrapure water, which ranged

**Table 1** Overview of characteristics of FITC-loaded nanoparticles. Results were calculated as the mean of three measurements followed by the standard deviations. Samples are coded

Formulation	dx(50) (nm)	Z-Ave (nm)	PdI	ZP (mV)	EE (%)	Conjugation efficiency SYSY 94 (%)	Conjugation efficiency control Ab (%)
0.2% PLGA FITC	319±4	n/a	n/a	-36.3±0.4	44.8±11	18.63±0.31	19.54±1.33
2% PLGA FITC	105±1	154±1	0.099	-37.2±0.7	12.2±0.7	13.31±0.39	14.12±1.07
2% PLGA-PEG-COOH FITC	86±9	245.1±0.4	0.424	-31.9±0.7	22.5±0.8	10.58±0.18	7.81±0.24
4% PLGA-PEG-COOH FITC	84±16	368±21	0.410	-34.6±1.2	28.4±1.9	1.82±0.14	n/a

by their formulation parameters: the amount of stabilizer used, indicating size class (0.2%–2%–4% PVA), and the (PEG) PLGA polymer used

from -31.9 to -37.2 mV. Furthermore, the EE was higher for the larger 0.2% PLGA NPs compared to 2% PLGA NPs. It should be noticed that PEG PLGA formulations also showed higher amounts of encapsulated dye. Generally, in vitro dye release profiles showed that the larger the particles, the slower the release (Fig. 1A). While the small 2% and 4% (PEG) PLGA NPs already reached their maximum burst release after 15 min (Fig. 1B), the large 0.2% NPs reached their maximum released amount after 420 min (7 h). Noteworthy is the fact that the release was incomplete for small-sized 2% and 4% (PEG) PLGA NPs as only ~90% of the dye was measured compared to ~98% for the larger 0.2% PLGA NPs. Remarkably for PEG PLGA NPs, FITC concentrations started declining after a few hours, as observed at time point 1440 min (24 h). At last, it should be noted that the starting points of the curves do not perfectly match with 0% released FITC (7–15%), corresponding to insufficient washing of the samples after production.

### Antibody production and conjugation

All purified and concentrated batches of the purified mAb SySy94 showed red surface staining on CHO-mSn cells after addition of the TRITC-conjugated secondary Ab. As expected, no surface staining for negative controls and on CHO-K cells could be detected. Therefore, the produced SySy94 antibodies were validated to be specific for the Sn receptor and were used for further conjugation to the NPs (Fig. 2).

Conjugation efficiencies ranged between undetectable concentrations for 4% PEG PLGA NPs to 19.54% for 0.2% FITC-loaded PLGA NPs. Overall,

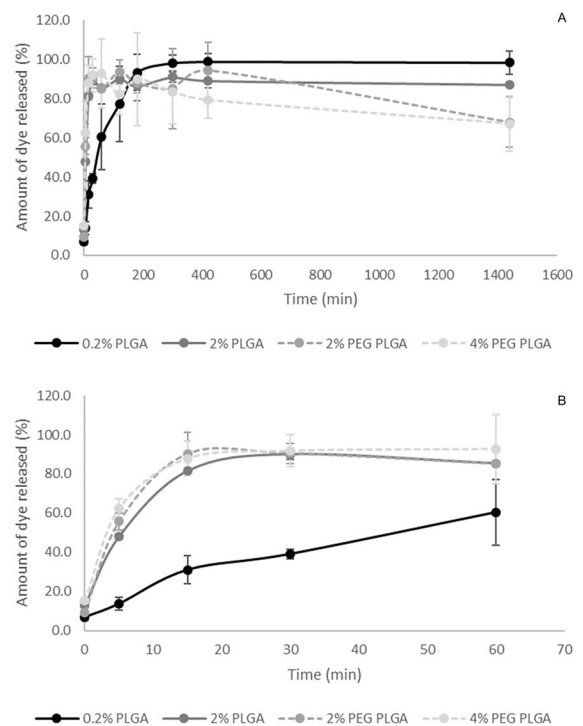
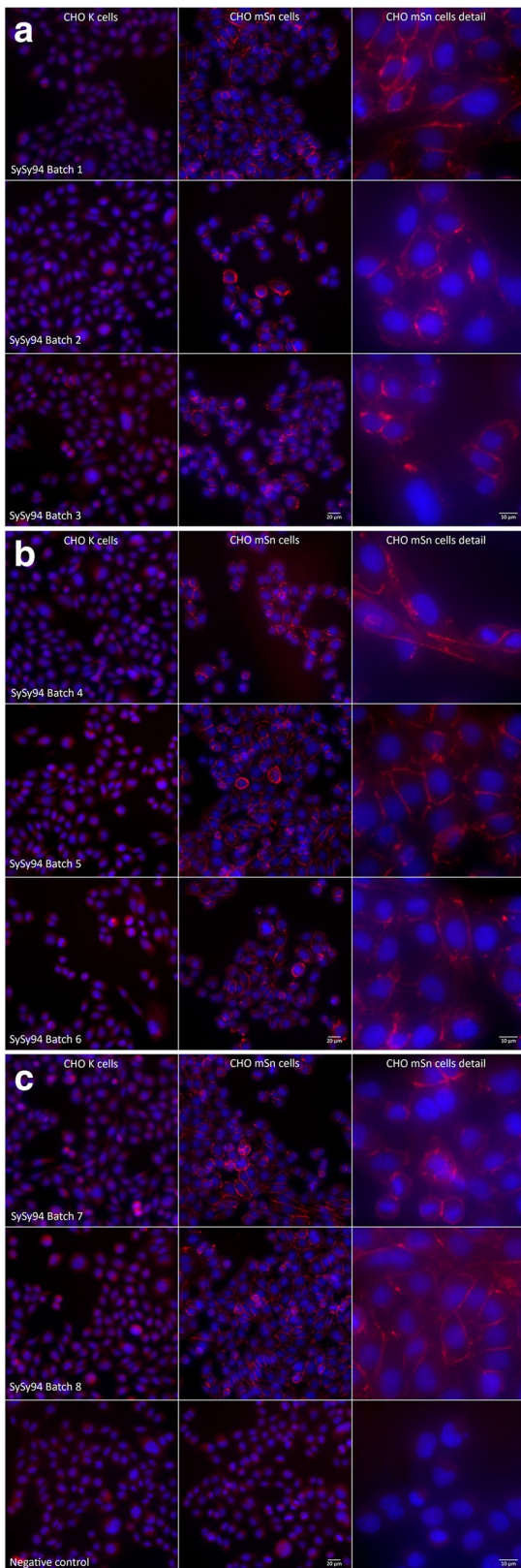


**Fig. 1** In vitro release profiles of the dye FITC from (PEG) PLGA nanoparticles over 24 h (A) and more in detail over 1 h (B). Results were calculated as the mean of three measurements, and error bars represent the standard deviation. Samples are coded by their formulation parameters: the amount of stabilizer used, indicating size class (0.2%–2%–4% PVA), and the used polymer: PLGA (solid line) or PEG PLGA (dashed lines)

**Fig. 2** Overview of surface staining pictures of CHO-murine sialoadhesion (mSn)-expressing cells and CHO-K (wildtype, control) cells treated with 8 produced batches of the SySy94 monoclonal antibody (mAb) and a TRITC-conjugated secondary mAb. The scale bars indicate 20 μm and 10 μm for the CHO-mSn detail images



the larger the NPs, the higher the antibody concentration that could be bounded to the surface. Results are presented in Table 1.

### Endocytosis assay of FITC encapsulated nanoparticles

While after 1 h of incubation, only a minor significant difference in MFI could be detected between 2% SySy94-conjugated PLGA NPs (dx(50) 105 nm) and the control NP group (Fig. 3A), after 4 h, the MFI of SySy94-conjugated NPs was significantly surpassing the MFI of control NPs and was higher, but not significantly different from the isotype control antibody-conjugated NPs. In addition, the percentage of fluorescent cells was significantly higher for SySy94-conjugated NPs compared to the other groups

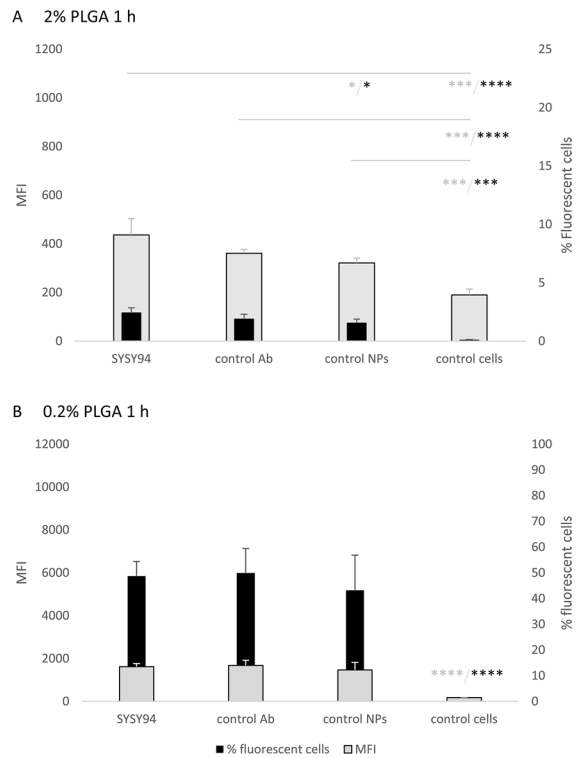


**Fig. 3** Analysis of FITC-loaded functionalized (SySy94, control antibody (cAb)) and unconjugated control nanoparticle’s uptake after 1-h incubation time by means of flow cytometry, including untreated macrophages (unstained). Small (2%) PLGA (A) and large (0.2%) PLGA (B) nanoparticles were evaluated for their mean fluorescence intensity (MFI, grey bars) and mean percentage fluorescent cells (black bars), calculated over three experiments. Error bars represent standard deviations. Asterisks represent level of significance

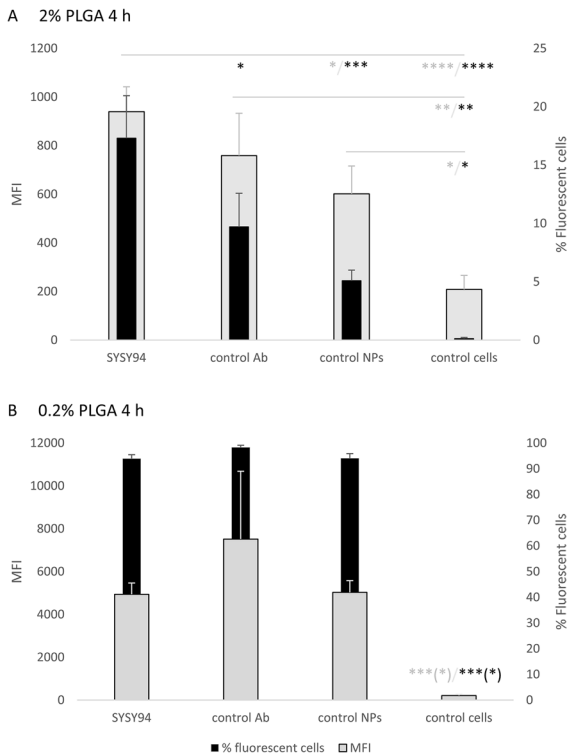


**Fig. 4** Summary of FITC-loaded functionalized (SySy94, control antibody (cAb)) and unconjugated control nanoparticle's uptake after 4-h incubation time by means of flow cytometry, including untreated macrophages (unstained). Small (2%) PLGA (A) and large (0.2%) PLGA (B) nanoparticles were evaluated for their mean fluorescence intensity (MFI, grey bars) and mean percentage fluorescent cells (black bars), calculated over three experiments. Error bars represent standard deviations. Asterisks represent the level of significance

(Fig. 4A). In contrast, for the large 0.2% NPs (dx(50) 319 nm), no difference could be perceived both after 1-h and 4-h incubation time (Figs. 3B and 4B).

Next, the uptake of different concentrations of all NP formulations after 24 h was evaluated. At this time, all formulations showed a percentage of fluorescent cells of about 99% and this outcome is therefore not shown.

For 2% PLGA NP formulations, Tukey HSD post hoc testing showed no significant difference in MFI between 2% SySy94-conjugated PLGA NPs and its control groups, taking the different tested concentrations into account (Fig. 5A). According to the statistic model, the low concentrations of added NPs differed significantly from the medium and high concentrations ( $p$ -values: 0.003 and  $2 \times 10^{-5}$

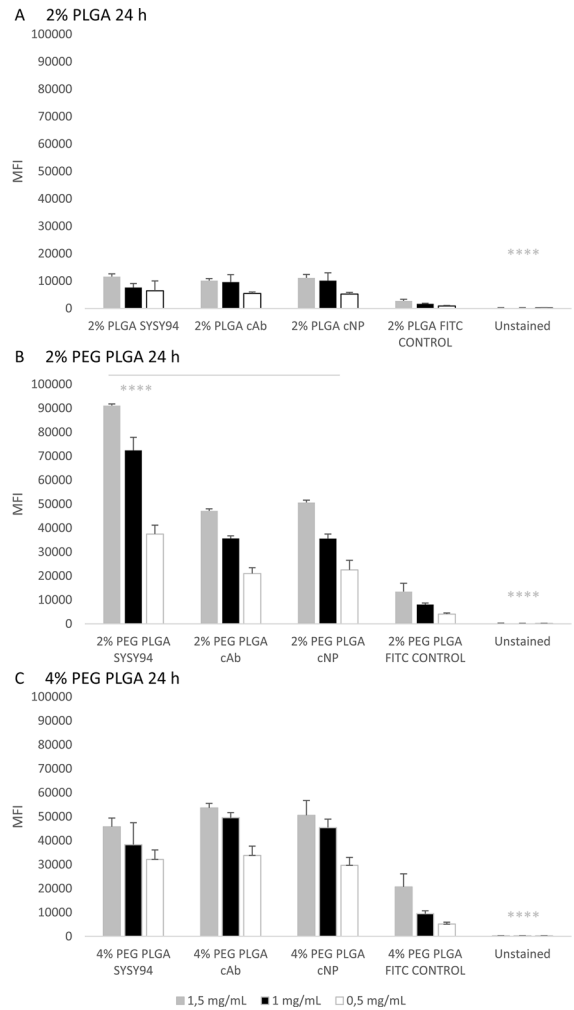
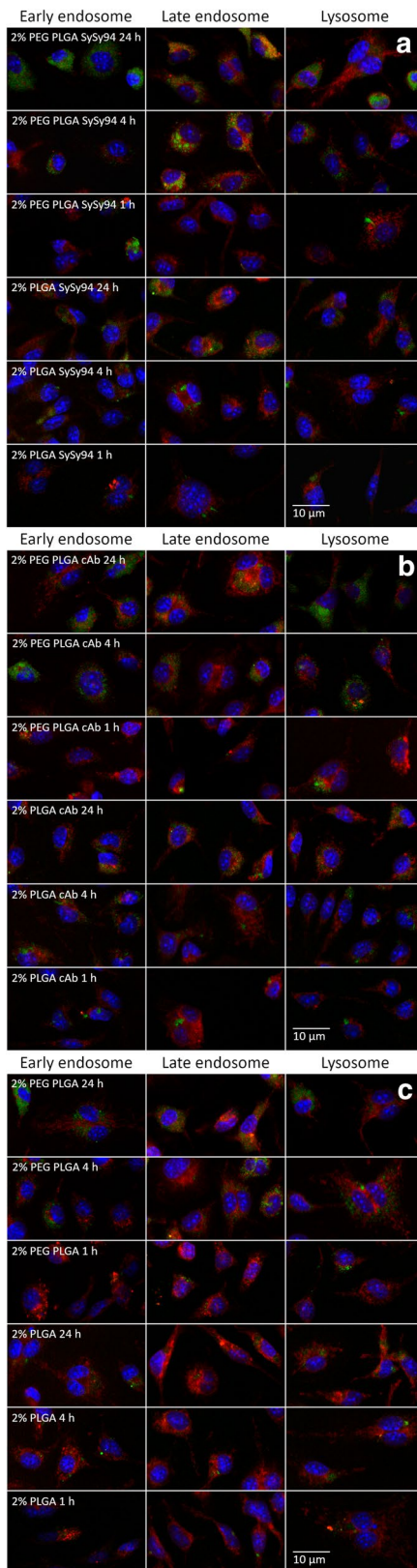


**Fig. 5** Effect of concentration of nanoparticles (mg/mL) of FITC-loaded functionalized (SySy94 and control antibody (cAb)) and unconjugated control nanoparticles (cNPs) on the uptake after 24-h incubation time by means of flow cytometry, in reference to the addition of the free FITC compound (FITC CONTROL) and untreated macrophages (unstained). Small (2%) PLGA (A) and small (2%) PEG PLGA (B) or very small (4%) PEG PLGA (C) nanoparticles were evaluated for their mean fluorescence intensity (MFI) calculated over three experiments. Error bars represent standard deviations. Asterisks represent the level of significance

**Fig. 6** Confocal fluorescence microscopy images of 2% SySy94-functionalized (PEG) PLGA nanoparticle's uptake and co-localization with early endosomes, late endosomes, and lysosomes in macrophages after 1-, 4-, and 24-h incubation time. Overall, no or minimal overlap in green and red color was observed. Colors indicate DAPI-stained blue cell nucleus, red Alexa Fluor 555-stained protein markers EEA1 for early endosomes, CI M6P for late endosomes, and cathepsin B for lysosomes and green FITC-containing nanoparticles. The scale bar indicates 10  $\mu$ m





respectively), and the medium and high concentrations amongst each other did not ( $p$ -value 0.133).

For 2% PEG PLGA NPs, the uptake was significantly higher for SySy94-conjugated NPs compared to the cAb-conjugated NPs and control NPs ( $p$ -values  $8 \times 10^{-13}$  for both) (Fig. 5B), while cAb-functionalized NPs did not differ from control NPs ( $p$ -value 0.501). Furthermore, all three groups of concentrations also differed significantly from each other.

For 4% PEG PLGA NPs, higher uptake, though not significant, was observed for isotype control antibody-conjugated NPs compared to SySy94-conjugated NPs and control NPs ( $p$ -value 0.0502 and 0.453 respectively) (Fig. 5C). No significant difference between SySy94-conjugated NPs and the control NPs ( $p$ -value 0.618) was present either. Moreover, low concentrations differed significantly from the medium and high concentrations ( $p$ -values: 0.001 and  $3 \times 10^{-6}$  respectively), while the medium and high concentrations again did not ( $p$ -value 0.155).

It should be noted that all formulations presented a major significant difference with untreated cells for MFI. The highest uptake efficiency based on MFI was obtained with the 2% PEG PLGA SYSY94 NPs at a concentration of 1 or 1.5 mg/mL of NPs.

### Fluorescence microscopy

As expected, the amount of green fluorescent particles inside the cells increased over time for all formulations. In line with the flow cytometry experiments, 2% PLGA NP-treated macrophages showed slightly less green staining compared to 2% PEG PLGA NPs. Although the formulations had different NP surfaces, the intracellular tracking of the NPs in macrophages revealed the absence of association between NP formulations and early endosomes, late endosomes, and lysosomes after the different incubation times of 1, 4, and 24 h (Fig. 6).

### Discussion

NP properties are characterized by the production process and the composition of the formulation (Qi et al. 2019). For example, due to the hydrophilic PEG-entities on the surface of the PEG PLGA formulations, the hydrodynamic diameter was larger compared to the diameters of the corresponding PLGA

**Table 2** Overview of how many times (the factor) higher MFI for FITC-loaded NPs was compared to free FITC control for the different formulations. This factor was approximately the same for all formulations when administered in the same concentration, except for 2% SYSY94-conjugated PEG PLGA NPs which was obviously higher (highlighted in bold, ital-

ics). Results were calculated as the mean of three measurements followed by the standard deviations. Samples are coded by three formulation parameters: (1) the amount of stabilizer used, indicating size class (0.2%–2%–4% PVA); (2) the (PEG) PLGA polymer used; (3) the functionalization of the NP surface

Formulation	Factor 0.5 mg/mL NPs	Factor 1 mg/mL NPs	Factor 1.5 mg/mL NPs
4% PEG PLGA SYSY 94	2.2±0.2	4.1±1.0	6.3±0.8
4% PEG PLGA cAb	2.6±0.1	5.2±0.2	6.6±0.8
4% PEG PLGA cNP	2.4±0.3	4.8±0.4	5.8±0.8
2% PEG PLGA SYSY 94	<b>6.8±0.1</b>	<b>8.9±0.7</b>	<b>9.2±0.9</b>
2% PEG PLGA cAb	3.5±0.1	4.4±0.1	5.2±0.6
2% PEG PLGA cNP	3.8±0.1	4.4±0.2	5.6±1.0
2% PLGA SYSY 94	4.2±0.4	4.6±0.9	6.9±0.4
2% PLGA cAb	3.7±0.3	5.8±1.6	5.9±0.6
2% PLGA cNP	4.1±0.5	6.1±1.7	5.6±0.7

preparations (Chen and Hu 2011; Suk et al. 2016). As for the production process, the washing and freeze-drying of the NPs had a substantial influence on the NP size and PdI, which were both considerably enlarged, presumably due to the formation of agglomerates (Vandervoort and Ludwig 2002). To compensate, all samples were sonicated prior to performing abovementioned experiments. Negative zeta potential values were obtained which correspond to the carboxylic end groups of both PLGA and PEG PLGA polymers.

For the EE, it was noticed that the larger the NPs, the higher the amount of encapsulated FITC. Logically, bigger spheres are able to contain more compound inside (Chen and Hu 2011). Peculiarly, a higher amount of FITC was encapsulated into PEG PLGA NPs compared to the complementary PLGA NPs. Hypothetically, FITC (a rather lipophilic compound) was hindered to a higher extent to pass the hydrophilic PEG barrier, and therefore, leakage of the compound out of the NPs was less present.

Similar to other studies, FITC release kinetics revealed fast burst release for FITC from the small 2%/4% NPs (Cheng et al. 2008) and slower leakage from 0.2% NPs (Yang et al. 2009). This is probably due to a larger diffusion distance that the dye has to cover inside the NPs before reaching the particle surface. It should be mentioned though that the total amount of released dye was quite high for all NPs as well as “complete” release of the dye happened quite

quickly (30 min and 7 h for small and large particles respectively). Another concern is the decline in the absorption after 24 h, noticeable for PEG PLGA formulations, which might be the result of FITC degradation due to acidic degeneration products from the polymer.

In previous research, an increase in total NP uptake in macrophages when coating PLGA NPs with chitosan derivatives was demonstrated (Van Hees et al. 2020). Therefore, it was unexpected that the functionalization of the PLGA NPs with specific antibodies against Sn did not lead to differences in total NP uptake for 2% FITC-loaded PLGA NPs after 24 h. As chitosan is presumably facilitating endocytosis through uptake via the mannose receptor (Vu-Quang et al. 2016; Durán et al. 2019), supposedly, the engulfment through the Sn receptor might be less efficient (Klaas and Crocker 2012).

After 1 and 4 h, the uptake of the smaller 2% SySy94-conjugated PLGA NPs was significantly higher compared to the control group(s). An increase in the uptake of cAb-conjugated PLGA NPs was also noticed after 4 h, hence to a lesser extent. It was previously observed that uptake rates of small PLGA NPs were low, but the total NP uptake after 24 h was high (Van Hees et al. 2020). Therefore, functionalization of these small-sized 2% PLGA NPs might have attributed to increased uptake rates for these formulations. In contrast, the larger 0.2% PLGA NPs, of which augmented uptake rates during the first hours

were formerly observed (Van Hees et al. 2020), did not show any differences in MFI between the groups after 1 and 4 h and were therefore discontinued from further experiments. Noticeably, the large isotype control antibody-conjugated PLGA NPs seemed to establish the highest uptake after 4 h, although no significant difference was present due to an outlier causing a large standard deviation.

It was decided to continue the 24-h assay with small-sized 4% and 2% PEG PLGA NPs instead of 0.2% PLGA NPs. PEG chains on PLGA NP surfaces are known to decrease NP uptake in macrophages (Suk et al. 2016). This strategy appeared to be successful, as a significant difference in MFI between 2% SySy94-conjugated PEG PLGA NPs and both control groups was present after 24 h for all assessed concentrations. Nonetheless, for NPs which were too appealing (e.g., 2% PLGA NPs) or too unattractive (e.g., 4% PEG PLGA NPs with low conjugation efficiency), no difference in MFI after 24 h could be perceived between SySy94-conjugated NPs and the control groups. A secondary effect of the isotype control antibody, binding through presumably the Fc receptor, was noticed for 4% PEG PLGA which showed an increase in FITC signal. In future experiments, replacing the antibody SySy94 with nanobodies or Fab fragments against sialoadhesin could contribute to a more selective formulation excluding the influence of the Fc ending of the antibody.

Remarkably, the absolute MFI values were considerably higher for PEG PLGA NPs compared to plain PLGA NPs, so it seems that contradictory to literature (Suk et al. 2016), PEG PLGA NPs were taken up to a higher extent compared to plain PLGA NPs. This can be (partially) explained by the higher EE for 4% PEG PLGA and 2% PEG PLGA NPs. Furthermore, when comparing the MFI of the NPs to their corresponding free FITC compound controls, the factor by which the MFI had increased was calculated. This factor was approximately the same for all formulations when administered in the same concentration, except for 2% SySy94-conjugated PEG PLGA NPs which was obviously higher (Table 2).

About the intracellular fate of PLGA NPs, many studies reported lysosomal entrapment of PLGA micro- and nanoparticles (Zhang et al. 2017; Kalluru et al. 2013; Pang et al. 2018; Schliehe et al. 2011), though no co-localization could be observed between

early endosomal, late endosomal, or lysosomal immuno-stained proteins and our (functionalized) NP formulations (2% PLGA and 2% PEG PLGA NPs) inside the cells. Similarly, other papers suggested escape of PLGA NPs to the cytoplasm or other cellular compartments (Gomes et al. 2006; Trombone et al. 2007; Lee et al. 2021; Yameen et al. 2014). Therefore, more research regarding the intracellular fate of our formulations is needed. Eshaghi et al. found that more rigid lipid-wrapped <sup>HMW</sup>PLA NPs were escaping to the CD9+ compartments inside macrophages while soft <sup>LMW</sup>PLA and ester-terminated PLGA NPs were prone to stay in lysosomal entities, regardless of GM3-surface functionalization (Eshaghi et al. 2020). In other research, it was also observed that surface functionalization had no influence on the presence of NPs in endo- nor lysosomal locality (Li et al. 2016), which might correspond to the hypothesis of Eshaghi et al. that other physicochemical properties, such as core stiffness, drive intracellular trafficking.

## Conclusion

In summary, SySy94-functionalized 2% FITC-loaded PEG PLGA NPs were found to be the better formulation for enhancing total nanoparticle uptake in macrophages. On the other hand, SySy94-conjugation also induced higher initial uptake rates for small-sized FITC-loaded PLGA NPs, although no benefits in the total uptake after 24 h could be established. Consequently, out of our data, it can be concluded that there was a positive effect on the uptake of SySy94-bound 2% (PEG) PLGA NPs compared to the control groups. Therefore, similarly to other studies (Chen et al. 2012; Nijen Twilhaar et al. 2020), targeting of Sn showed to be an effective strategy for improving NP uptake, but was found to be time- and formulation-dependent.

To conclude, enhancing nanoparticle uptake in primary bone marrow-derived macrophages is possible through conjugation of antibodies targeting Sn. However, the degree of uptake in these cells is time- and formulation-dependent. Furthermore, NPs were not found in association with endosomal or lysosomal proteins and no difference in intracellular fate of the various (functionalized) formulations could be observed.

**Acknowledgements** The authors wish to thank the staff of The Laboratory of Microbiology, Parasitology, and Hygiene of the University of Antwerp for their technical assistance and expertise during experiments. We'd like to acknowledge Pim-Bart Feijens for the isolation of macrophages. We'd very much like to thank Dr. Isabel Pintelon and Sofie Thys for the confocal microscopy images.

**Author contribution** Sofie Van Hees: Conceptualization, methodology, formal analysis and investigation, writing — original draft preparation, visualization.

Kimberley Elbrink: Formal analysis and investigation, writing — review & editing.

Marjorie De Schryver: Methodology and investigation, writing — review & editing.

Peter Luc Delputte: Conceptualization, resources, writing — review & editing, supervision.

Filip Kiekens: Conceptualization, resources, writing — review & editing, supervision.

**Data availability** Not applicable.

**Code availability** Not applicable.

## Declarations

**Ethics approval** Cells were obtained from control female Swiss mice whereof experiments were authorized by the Ethical Committee for Animals of the University of Antwerp, permit number 2019–10.

**Conflict of interest** The authors declare no competing interests.

## References

- Asano K, Kikuchi K, Tanaka M (2018) CD169 macrophages regulate immune responses toward particulate materials in the circulating fluid. *J Biochem* 164(2):77–85
- Chen W, Hu S (2011) Suitable carriers for encapsulation and distribution of endostar: comparison of endostar-loaded particulate carriers. *Int J Nanomedicine* 6(6):1535–1541
- Chen WC, Kawasaki N, Nycholat CM et al (2012) Antigen delivery to macrophages using liposomal nanoparticles targeting Sialoadhesin/CD169. *PLoS ONE* 7(6):1–9
- Cheng FY, Wang SPH, Su CH et al (2008) Stabilizer-free poly(lactide-co-glycolide) nanoparticles for multimodal biomedical probes. *Biomaterials* 29(13):2104–2112
- Delputte PL, van Gorp H, Favoreel HW et al (2011) Porcine sialoadhesin (CD169/Siglec-1) is an endocytic receptor that allows targeted delivery of toxins and antigens to macrophages. *PLoS ONE* 6(2):1–12
- De Schryver M, Cappoen D, Elewaut D et al (2017b) Monoclonal antibody binding to the macrophage-specific receptor sialoadhesin alters the phagocytic properties of human and mouse macrophages. *Cell Immunol* 312:51–60
- De Schryver M, Leemans A, Pintelon I et al (2017a) Comparative analysis of the internalization of the macrophage receptor sialoadhesin in human and mouse primary macrophages and cell lines. *Immunobiology* 222(6):797–806
- De Schryver M, Van Gorp H, Hoebeke I et al (2016) Development and characterization of new species cross-reactive anti-sialoadhesin monoclonal antibodies. *Antibodies* 5(7):1–18
- Durán V, Yasar H, Becker J et al (2019) Preferential uptake of chitosan-coated PLGA nanoparticles by primary human antigen presenting cells. *Nanomedicine Nanotechnol Biol Med* 21:102073
- Elmowafy EM, Tiboni M, Soliman ME (2019) Biocompatibility, biodegradation and biomedical applications of poly (lactic acid)/ poly (lactic-co-glycolic acid) micro and nanoparticles. *J Pharm Investig* 49(4):347–380
- Eshaghi B, Alsharif N, An X et al (2020) Stiffness of HIV-1 Mimicking polymer nanoparticles modulates ganglioside-mediated cellular uptake and trafficking. *Adv Sci* 7(18):1–13
- Gaspar N, Zambito G, Mezzanotte L (2019) Active nano-targeting of macrophages. *Curr Pharm Des* 25:1951–1961
- Gomes AJ, Faustino AS, Machado AEH et al (2006) Characterization of PLGA microparticles as a drug carrier for 3-ethoxycarbonyl-2H-benzofuro[3,2-f]-1-benzopyran-2-one. Ultrastructural study of cellular uptake and intracellular distribution. *Drug Deliv* 13(6):447–454
- Hartnell A, Steel J, Turley H, Jones M, Jackson DG, Crocker PR (2001) Characterization of human sialoadhesin, a sialic acid binding receptor expressed by resident and inflammatory macrophage populations. *Blood* 97(1):288–296
- Hu J, Wei P, Seeberger PH, Yin J (2018) Mannose-functionalized nanoscaffolds for targeted delivery in biomedical applications. *Chem - an Asian J* 13(22):3448–3459
- Jain NK, Mishra V, Mehra NK (2013) Targeted drug delivery to macrophages. *Expert Opin Drug Deliv* 10(3):353–367
- Jones C, Virji M, Crocker PR (2003) Recognition of sialylated meningococcal lipopolysaccharide by siglecs expressed on myeloid cells leads to enhanced bacterial uptake. *Mol Microbiol* 49(5):1213–1225
- Kalluru R, Fenaroli F, Westmoreland D et al (2013) Poly(lactide-co-glycolide)-rifampicin nanoparticles efficiently clear mycobacterium bovis BCG infection in macrophages and remain membrane-bound in phago-lysosomes. *J Cell Sci* 126(14):3043–3054
- Kelly C, Jefferies C, Cryan S-A (2011) Targeted liposomal drug delivery to monocytes and macrophages. *J Drug Deliv* 2011:727241
- Klaas M, Crocker PR (2012) Sialoadhesin in recognition of self and non-self. *Semin Immunopathol* 34(3):353–364
- Lee SY, Fierro JJ, Tran AM, Hong D, Espinal J, Dou H (2021) Cytoplasmic trafficking of nanoparticles delivers plasmid DNA for macrophage gene-editing. *Curr Gene Ther* 21:1–12
- Li Z, Xiong F, He J, Dai X, Wang G (2016) Surface-functionalized, pH-responsive poly(lactic-co-glycolic acid)-based microparticles for intranasal vaccine delivery: effect of surface modification with chitosan and mannan. *Eur J Pharm Biopharm* 109:24–34

- Nijen Twilhaar MK, Czentner L, Grabowska J et al (2020) Optimization of liposomes for antigen targeting to splenic cd169+ macrophages. *Pharmaceutics* 12(12):1–21
- O'Neill ASG, Van Den Berg TK, Mullen GED (2013) Sialoadhesin - a macrophage-restricted marker of immunoregulation and inflammation. *Immunology* 138(3):198–207
- Ohnishi K, Komohara Y, Saito Y et al (2013) CD169-positive macrophages in regional lymph nodes are associated with a favorable prognosis in patients with colorectal carcinoma. *Cancer Sci* 104(9):1237–1244
- Ooms K, Van Gorp H, Van Gaever T, Nauwynck HJ, Delputte PL (2013a) Development of a recombinant antibody to target peptides and proteins to sialoadhesin-expressing macrophages. *BMC Biotechnol* 13(33):1–10
- Ooms K, Van Gorp H, Botti S, Van Gaever T, Delputte PL, Nauwynck HJ (2013b) Evaluation of viral peptide targeting to porcine sialoadhesin using a porcine reproductive and respiratory syndrome virus vaccination-challenge model. *Virus Res* 177(2):147–155
- Pang L, Zhu Y, Qin J, Zhao W, Wang J (2018) Primary M1 macrophages as multifunctional carrier combined with PLGA nanoparticle delivering anticancer drug for efficient glioma therapy nanoparticle delivering anticancer drug for efficient glioma therapy. *Drug Deliv* 25(1):1922–1931
- Patra JK, Das G, Fraceto LF et al (2018) Nano based drug delivery systems : recent developments and future prospects. *J Nanobiotechnology* 16(71):1–33
- Pei Y, Yeo Y (2016) Drug delivery to macrophages: challenges and opportunities. *J Control Release* 240:202–211
- Qi F, Wu J, Li H, Ma G (2019) Recent research and development of PLGA/PLA microspheres/nanoparticles: a review in scientific and industrial aspects. *Front Chem Sci Eng* 13(1):14–27
- Schliehe C, Schliehe C, Thiry M et al (2011) Microencapsulation of inorganic nanocrystals into PLGA microsphere vaccines enables their intracellular localization in dendritic cells by electron and fluorescence microscopy. *J Control Release* 151(3):278–285
- Suk JS, Xu Q, Kim N, Hanes J, Ensign LM (2016) PEGylation as a strategy for improving nanoparticle-based drug and gene delivery. *J Control Release* 228:1–13
- Trombone APF, Silva CL, Almeida LP et al (2007) Tissue distribution of DNA-Hsp65/TDM-loaded PLGA microspheres and uptake by phagocytic cells. *Genet Vaccines Ther* 5:1–8
- Vandervoort J, Ludwig A (2002) Biocompatible stabilizers in the preparation of PLGA nanoparticles: a factorial design study. *Int J Pharm* 238:77–92
- Van Hees S, Elbrink K, De Schryver M, Delputte PL, Kiekens F (2020) Improving cellular uptake and cytotoxicity of chitosan-coated poly(lactic-co-glycolic acid) nanoparticles in macrophages. *Nanomedicine* 15(27):2671–2688
- Vu-Quang H, Vinding MS, Xia D et al (2016) Chitosan-coated poly(lactic-co-glycolic acid) perfluorooctyl bromide nanoparticles for cell labeling in 19F magnetic resonance imaging. *Carbohydr Polym* 136:936–944
- Wagh A, Law B (2013) Chapter 15 methods for conjugating antibodies to nanocarriers. In: Ducry L (ed) *Antibody-drug conjugates, methods in molecular biology*, vol 1045. Springer Science+Business Media, LLC. [https://doi.org/10.1007/978-1-62703-541-5\\_15](https://doi.org/10.1007/978-1-62703-541-5_15)
- Yameen B, Choi WI, Vilos C, Swami A, Shi J, Farokhzad OC (2014) Insight into nanoparticle cellular uptake and intracellular targeting. *J Control Release* 190:485–499
- Yang H, Lj K, Liu Y, Liu Z, Miyoshi H (2009) Poly(D, L-lactide-co-glycolide) nanoparticles encapsulated fluorescent isothiocyanate and paclitaxol: preparation, release kinetics and anticancer effect. *J Nanosci Nanotechnol* 9(1):282–287
- Zhang J, Chang D, Yang Y et al (2017) Systematic investigation on the intracellular trafficking network of polymeric nanoparticles. *Nanoscale* 9(9):3269–3282

**Publisher's note** Springer Nature remains neutral with regard to jurisdictional claims in published maps and institutional affiliations.